



Cite this: Dalton Trans., 2024, 53, 9590

Received 22nd March 2024,  
Accepted 5th May 2024

DOI: 10.1039/d4dt00853g  
rsc.li/dalton

## On the mechanism of $sp^2$ C–H borylation using *ortho*-N-substituted pyridinium cations†

Nikita Slesarchuk, Enlu Ma,<sup>a</sup> Juan Miranda-Pizarro,<sup>a</sup> Sami Heikkinen,<sup>a</sup> Dieter Schollmeyer,<sup>b</sup> Martin Nieger,<sup>a</sup> Petra Vasko and Timo Repo <sup>a\*</sup>

*ortho*-N-Substituted pyridinium cations with the weakly coordinating anion  $[B(C_6F_5)_4]^-$  have been studied and crucial structural features in the  $sp^2$  C–H borylation catalysis of 3-methylthiophene have been identified. The electron-deficiency of the aromatic core of the cation is essential for activity together with accessible protons. The spectroscopic yield of the borylation of 3-methylthiophene with catecholborane (CatBH) was optimized up to 86% and the method was further applied to other substrates such as *N*-alkylbenzenes. A mechanistic DFT study revealed the rate-limiting step in the catalysis to be the liberation of molecular  $H_2$  ( $\Delta G^\ddagger = 27.5$  kcal mol<sup>-1</sup>), whereas the overall reaction was found to be exergonic by 5.1 kcal mol<sup>-1</sup>.

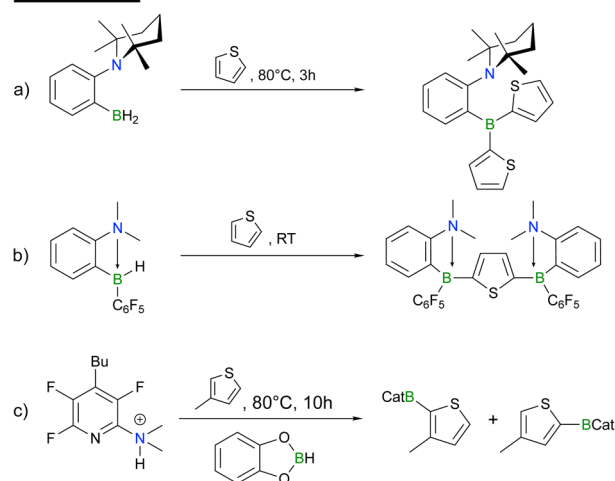
## Introduction

C–H borylation of an  $sp^2$  carbon is one of the most desired yet arduous chemical transformations.<sup>1,2</sup> It is an effective way to access useful building blocks for further cross-coupling reactions. For example, taking advantage of boronic ester precursors, the Suzuki–Miyaura coupling ensures that many important pharmaceuticals become available.<sup>3</sup> Currently,  $sp^2$  C–H borylation is accessible with platinum-group metal catalysts.<sup>1,2</sup> Due to the low Earth-abundance of precious metals and meticulous removal of metal traces in the final product, the demand for metal-free borylation is growing.<sup>4</sup> In fact, metal-free  $sp^2$  C–H borylations are not yet numerous but have already proven to be highly effective.<sup>5–14</sup>

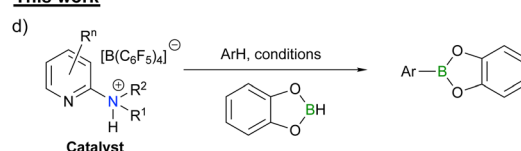
Metal-free, boron-based catalysts for  $sp^2$  C–H borylation take advantage of either the Frustrated Lewis Pair (FLP) approach or the high reactivity of borenium cations. Both strategies can facilitate the heterolytic splitting of  $H_2$ ,<sup>15–22</sup> binding of  $CO_2$ <sup>23–26</sup> and even breakage of some C–H bonds.<sup>5–9,12,13,27–29</sup> Indeed, our group has recently reported that *ortho*-TMP- $C_6H_4$ -BH<sub>2</sub> (TMP = 2,2,6,6-tetramethylpiperid-1-yl) (Scheme 1a) is capable of stoichiometrically activating the  $sp^2$  C–H bond of thiophene at elevated temperatures, whereas the bulkier *ansa*-aminoborane with an electron withdrawing

$C_6F_5$ -substituent on the boron can react even at room temperature (Scheme 1b).<sup>5</sup> Moreover, it has been shown that a 2-dimethylaminopyridinium cation with a weakly coordinating

### Previous work



### This work



**Scheme 1** (a)  $sp^2$  C–H activation of thiophene by *ortho*-TMP- $C_6H_4$ -BH<sub>2</sub>;<sup>5</sup> (b)  $sp^2$  C–H activation of thiophene by *ortho*-Me<sub>2</sub>N- $C_6H_4$ -BHC<sub>6</sub>F<sub>5</sub>;<sup>5</sup> (c) catalytic borylation of 3-methylthiophene;<sup>5</sup> (d) general reaction scheme of the borylation based on the pyridinium core used in this work.

<sup>a</sup>Department of Chemistry, Laboratory of Inorganic Chemistry, University of Helsinki, P.O. Box 55, FIN-00014, Finland. E-mail: timo.repo@helsinki.fi

<sup>b</sup>Johannes Gutenberg-Universität Mainz, Department Chemie, Duesbergweg 10-14, D-55099 Mainz, Germany

†Electronic supplementary information (ESI) available: Experimental procedures, NMR spectra, results of supplementary experiments, and computational details. CCDC 2288120 (3a). For ESI and crystallographic data in CIF or other electronic format see DOI: <https://doi.org/10.1039/d4dt00853g>



$[\text{B}(\text{C}_6\text{F}_5)_4]^-$  anion can catalytically borylate 3-methylthiophene with catecholborane (Scheme 1c).<sup>5</sup> Besides the 2-dimethylaminopyridinium salt, there are several other examples of catalytic metal-free  $\text{sp}^2$  C–H activation of different arenes and heterocycles using FLP or borenium catalysts.<sup>6–9,12–14</sup> However, most examples have different shortcomings such as high air- and/or moisture-sensitivity, limitations to use only electron-rich heteroarene substrates or poor accessibility to the catalyst.

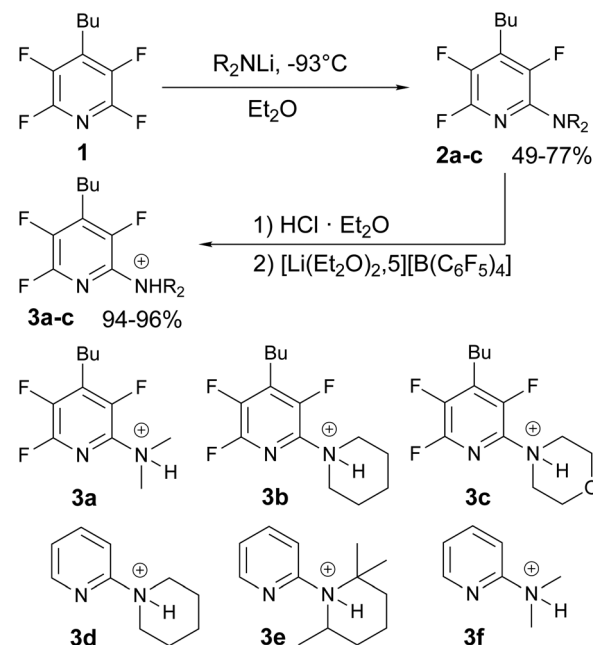
Herein, we report on the investigations of the structure-reactivity relationships and mechanistic understandings of the bench-stable 2-dimethylaminopyridinium derived catalyst, expand the substrate scope of the catalysis and discuss on the limitations of assembling CatB-derivatives from bench-stable pyridin-2-ylaminiums (Scheme 1d).

## Results and discussion

### Synthesis and optimization

In our previous research, we proposed that an *o*-*N*-substituted pyridinium cation, together with different hydroboranes, can liberate molecular hydrogen to form a compound that is reminiscent of an *ansa*-aminoborane-type FLP while also exhibiting borenium cation characteristics.<sup>5</sup> Here the Lewis base component of the FLP directly affects the reactivity, which is clearly demonstrated in the previous reports.<sup>8,18</sup> Hence, a systematic study of the effects of the *o*-*N*-substituent in the cation framework was first considered. Different *o*-*N*-substituted pyridinium compounds can be easily accessed from one precursor; our synthetic route<sup>5</sup> was slightly modified from the previously reported to yield *p*-butyltetrafluoropyridine **1** (Scheme 2). Next, we could introduce different secondary amines in the *ortho*-position of **1** to yield compounds **2a–c**. In the final step, a reported procedure<sup>5</sup> was applied towards aminopyridines in order to synthesise the targeted salts incorporating the weakly coordinating anion  $[\text{B}(\text{C}_6\text{F}_5)_4]^-$  (**3a–c**). In a search for more simplified cations, other pyridine-based derivatives (**3d–f**) were also synthesized (see detailed syntheses in the ESI†). Compounds **1–3** were characterised in solution by multinuclear NMR spectroscopy to confirm the successful syntheses of the compounds (see the ESI†). In the case of **3a** we were able to grow single crystals that were suitable for single-crystal X-ray diffraction studies. Crystals grown from a mixture of hexane/DCM (5 : 1) confirmed the molecular structure of **3a** to be an ionic species where the acidic proton is located on the dimethylamino group rather than on the pyridyl nitrogen (Fig. 1).

To optimize the reaction conditions for the  $\text{sp}^2$  C–H borylation, 3-methylthiophene was chosen as the substrate and **3a** as the catalyst (Table 1). The solvent screening (entries 1–5) revealed that aromatic solvents such as  $\text{C}_6\text{D}_6$  and PhBr facilitate high conversions, although toluene appeared to be less effective than a neat reaction (entry 1 vs. 3). 1,2-Dichloroethane (DCE) resulted in moderate conversion, together with higher selectivity for 2-BCat-3-methylthiophene (see the ESI†). The reaction described in entry 7 was conducted



**Scheme 2** General scheme of the syntheses of the catalysts **3a–c**.  $\text{R}_2\text{NLi}$  for **2b–c** was prepared *in situ*. **2,3a**:  $\text{R} = \text{Me}$ ; **2,3b**:  $\text{R}_2 = -(\text{CH}_2)_5-$ ; **2,3c**:  $\text{R}_2 = -(\text{CH}_2)_2\text{O}(\text{CH}_2)_2-$ . The  $[\text{B}(\text{C}_6\text{F}_5)_4]^-$  anion is omitted. All described compounds were characterized by NMR and HRMS (see the ESI†).

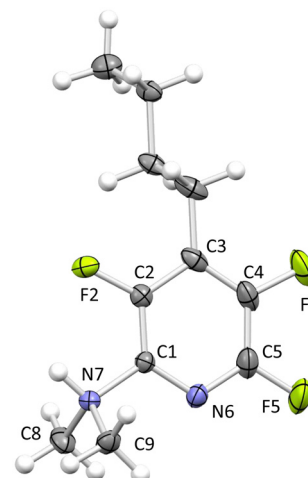


**Fig. 1** Molecular structure of the cation of **3a**. The  $[\text{B}(\text{C}_6\text{F}_5)_4]^-$  anion is omitted for clarity. Displacement parameters are drawn at 50% probability level. Selected bond lengths (Å) and angles (°):  $\text{C}1–\text{N}7 = 1.470(5)$ ;  $\text{C}1–\text{N}6 = 1.322(5)$ ;  $\text{N}7–\text{C}9 = 1.499(5)$ ;  $\text{N}7–\text{C}8 = 1.513(5)$ ;  $\text{N}6–\text{C}1–\text{N}7 = 115.1(3)$ ;  $\text{C}9–\text{N}7–\text{C}8 = 111.6(3)$ .

by adding a second equivalent of catecholborane to entry 4 and heating for another 24 hours. In this case, the conversion improved significantly. To investigate the optimal time for the reaction, two samples prepared at the same time were heated either at 80 or 110 °C and monitored by  $^1\text{H}$  and  $^{11}\text{B}$  NMR spectroscopy at selected time points (see the ESI†). An increase in



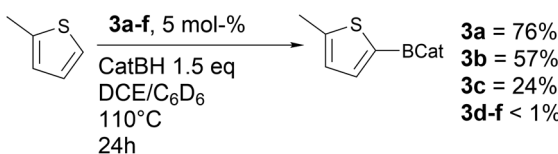
**Table 1** Optimization of the  $sp^2$  C–H borylation of 3-methylthiophene with catalyst **3a**<sup>a</sup>

#	Temp. (°C)	Solvent	CatBH (eq.)	<b>3a</b> (mol%)	Time (h)	Conv. (%)
1	80	PhMe	1	4	24	54
2	80	PhBr	1	4	24	87.5
3	80	Neat	1	4	24	69
4	80	$C_6D_6$	1	4	24	74
5	80	DCE	1	4	24	63
6	80	Neat	2	4	120	65
7	80	$C_6D_6$	2	4	48	95
8	110	$C_6D_6$	1	0.1	24	9
9	110	$C_6D_6$	1	1	24	37
10	110	$C_6D_6$	1	5	24	82
11	110	$C_6D_6$	1	10	24	89
12	110	$C_6D_6$	1	0.1	120	21
13	110	$C_6D_6$	1	1	120	81
14	110	DCE	1	5	24	78
15	110	DCE	1.5	5	24	88
16	110	DCE	2	5	24	87
17	110	DCE	5	5	24	91

<sup>a</sup> All reactions were carried out in J. Young NMR tubes. For detailed reaction conditions, see the ESI.†

conversion was observed even beyond 24 hours, which indicates a high thermal stability of the catalyst. Finally, the catalyst loading was screened (entries 8–13) and an optimal conversion was observed at 5 mol% loading. In the entries 12 and 13, a significant increase in conversion was observed compared to entries 8 and 9, where the time was increased up to 120 hours, which again indirectly confirms the stability of the catalytic system. The last step of the optimization focussed on the screening of the amount of catecholborane, finding 1.5 equivalents to be ideal; thus entry 15 presents the optimised conditions used in the catalytic studies (*vide infra*).

Subsequent screening of the catalysts **3a–c** unfolded that replacement of the *ortho*-N-substituent from a dimethylamino- (**3a**) to piperidino- or morpholino-substituent (**3b** and **3c**, respectively) decreased the yields of C–H borylation of 2-methylthiophene (Scheme 3). Interestingly, Fontaine *et al.* have reported that *o*-piperidino- $C_6H_4$ –BH<sub>2</sub> is a faster catalyst than *o*-NMe<sub>2</sub>- $C_6H_4$ –BH<sub>2</sub>.<sup>8</sup> Apparently, in the case of the amino-



**Scheme 3** Catalyst screening for the borylation of 2-methylthiophene. All reactions were carried out in J. Young NMR tubes. NMR yields were calculated based on HMB as an internal standard (HMB = hexamethylbenzene).

pyridinium salts, *o*-N-substituent has only an auxiliary role in the C–H borylation. Non-fluorinated derivatives **3d–f** showed only traces of borylated products under the same conditions and a very small conversion of 3-methylthiophene. It is likely that the electron-withdrawing effect of fluorine is essential in this type of catalysis.

## Substrate scope

The optimized reaction conditions were applied to a variety of substrates (Fig. 2), including those that are particularly averse to borylation. In the selected conditions, methylthiophenes can be borylated up to 76% spectroscopic yield (**4a**, **4b**). The reaction also proceeds in the case of unsubstituted thiophene (**4c**) and benzothiophene (**4d**), but with low yields. Using *N*-phenylpyrrole as the substrate, we found that a complete reduction of the pyrrole ring and borylation occurred simultaneously (**4f**, Fig. 2b). Here we suggest that the

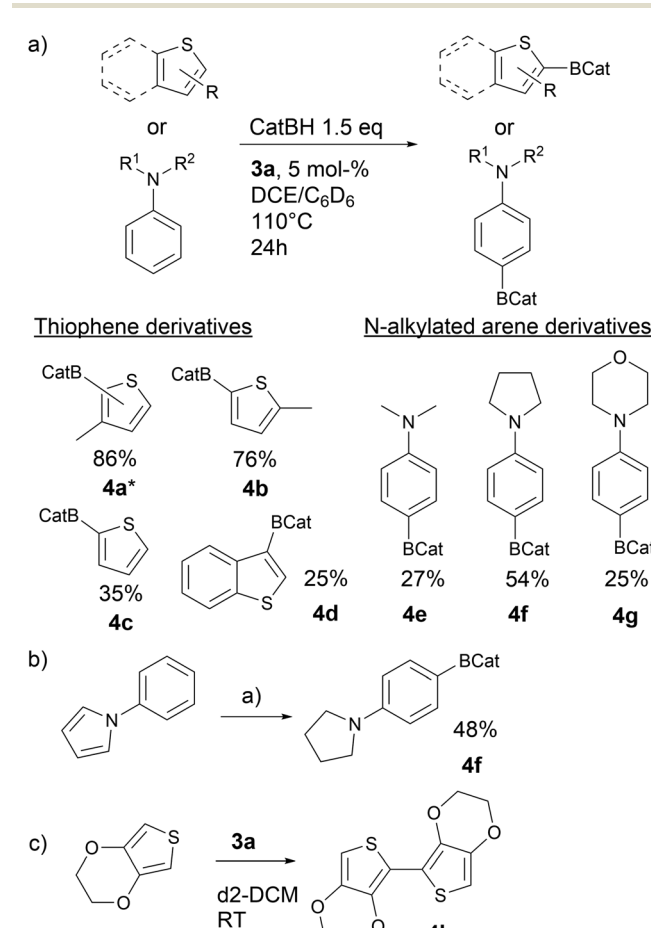


**Fig. 2** Substrate scope for borylation under the optimized conditions with **3a**. All reactions were carried out in J. Young NMR tubes. NMR yields were calculated based on HMB as an internal standard. For detailed experimental data see the ESI.† (a)  $sp^2$  C–H borylation of thiophene and *N*-alkylated derivatives; (b) reduction and  $sp^2$  C–H borylation of *N*-phenylpyrrole; (c) oligomerization of 3,4-ethylenedioxythiophene.<sup>30</sup> \* The selectivity of the 2-Bcat-product and 5-Bcat-product is 73:13.



*N*-phenylpyrrole is first reduced to *N*-phenylpyrrolidine after which borylation occurs. This pathway can be supported by the following facts; firstly, C–H borylation proceeds with phenyl-*N*-pyrrolidine; secondly, our system releases H<sub>2</sub> (*vide infra*) and thirdly, pyrroles are acidophobic species.

We also tested *N*-substituted benzenes as substrates (**4e–4g**) where a pyrrolidinobenzene derivative (**4f**) was the most affordable with 54% spectroscopic yield. The lower yields in the two other cases can be explained by the less activated ring (aniline **4e**) and the presence of oxygen (morpholine **4g**), which can interfere with the borane species and hamper the desired reactivity. We also tested the electron-rich 3,4-ethylenedioxythiophene (Fig. 2c) observing a colour change from yellow to orange and eventually to deep blue upon adding the catalyst to the substrate solution. Apparently, the catalyst is acidic enough to protonate this substrate directly and triggers its oligomerization instead of borylation.<sup>30</sup> 2-Bromo- and 3-bromo thiophenes do not result in any products of borylation upon similar conditions, due to the electron-withdrawing effects of the bromide. Upon using pinacolborane (PinBH) as the boron source, ring-opening of the PinBH occurred in the same way as previously described,<sup>12</sup> indirectly proving the high acidity of the catalyst **3a**.

### Borylation mechanism

To gain more insight into the mechanism of the sp<sup>2</sup> C–H borylation, we continued our experiments with **3a** as the catalyst and 3-methylthiophene as the substrate. When **3a** is mixed with a stoichiometric amount of CatBH at RT, the <sup>1</sup>H NMR spectrum of the mixture reveals a signal for molecular hydrogen and a new broad singlet can be found at 7.9 ppm along with aromatic signals originating from CatBH (see the ESI†). Here, additional 2D NMR experiments were performed to gain a better understanding of the reaction. The same mixture was cooled to –23 °C and the obtained data revealed cross-signals between the broad singlet at 7.9 ppm and the dimethylamino group in the COSY and NOESY spectra (in the negative area). Thus, the acidic proton is still located close to the dimethylamino group of the cation even upon mixing with CatBH. However, both species interact with each other, resulting in the liberation of H<sub>2</sub> and decomposition of CatBH to CatB-oligomers which is evident in the <sup>11</sup>B and <sup>1</sup>H NMR spectra. Previously, this was attributed to Cat<sub>3</sub>B<sub>2</sub>.<sup>5</sup> The formation of Cat<sub>3</sub>B<sub>2</sub> together with BH<sub>3</sub>·L could occur following the Marder mechanism when CatBH is exposed to a Lewis base.<sup>31</sup> However, this mechanism does not imply H<sub>2</sub> formation and during our experimental work there was no evidence of formation of BH<sub>3</sub>. Apparently, the reaction of **3a** with **CatBH** includes a second, competing pathway for the formation of H<sub>2</sub> during the stoichiometric NMR studies. This observation follows the optimization study where 1.5 equiv. of CatBH were found to be optimal for the catalysis. After 24 h, the mixture of CatBH and **3a** (1:1) includes the various CatB-oligomers which cannot react with 3-methylthiophene, even upon heating at 110 °C. Whereas these side reactions take place in RT, the borylation of 3-methylthiophene proceeds at higher temperatures.

Computational investigations using density functional theory (DFT) at the PBE1PBE-GD3BJ/Def2-TZVP level of theory were undertaken to clarify the mechanism of the C–H borylation further. In the calculations, we omitted the effect of the weakly coordinating anion and focused only on the cationic part of **3a** (see the ESI† for full computational details). The cation in **3a** and CatBH interact only weakly, but when in correct orientation, molecular hydrogen can be liberated. The activation barrier for hydrogen release (**TS1** in Fig. 3) was calculated to be 27.5 kcal mol<sup>–1</sup>, which is in agreement with the experimental observations of obtaining borylation only at high reaction temperatures (80–110 °C). The high barrier also confirms that the liberation of H<sub>2</sub> observed in the stoichiometric reactions performed at RT occurs *via* a different pathway producing the CatB-oligomers.

The formation of intermediate **Int1** is calculated to be exergonic by 3.1 kcal mol<sup>–1</sup>. The structure of **Int1** is analogous to the one calculated by Ingleson and co-workers, who reported the effective haloboration of internal alkynes by cationic boronium and borenium compounds.<sup>32</sup> Identifying the relative energy of **Int1** compared to the starting materials, we tried to isolate it experimentally *via* a hydride cleavage of CatBH in the presence of **2a** and BCF. Upon mixing **2a**, BCF and CatBH (1:1:1), we observed an equilibrium between CatBH, **2a** and the adduct [CatBH-**2a**] (see the ESI†). However, this mixture did not afford the **Int1** cation and [HB(C<sub>6</sub>F<sub>5</sub>)<sub>3</sub>]<sup>–</sup> anion, which are usually formed in combination with other Lewis bases, CatBH and BCF.<sup>33</sup> Furthermore, it is known that at elevated temperatures BCF and CatBH react forming CatBC<sub>6</sub>F<sub>5</sub> which is detrimental to the catalysis.<sup>12</sup>

The high calculated barrier for the H<sub>2</sub> liberation prompted us to test whether the required activation energy could be lowered by mixing **2a**, **3a** and CatBH (1:1:1) in order to form **Int1** through liberation of H<sub>2</sub> from **3a** and [CatBH-**2a**]. However, the NMR spectra of the mixture revealed no new signals that could be attributed to **Int1**. Apparently, intramolecular liberation of H<sub>2</sub> *via* **TS1** is more accessible in this case compared to an intermolecular H<sub>2</sub> liberation from [CatBH-**2a**] and **3a**.

The next step in the calculated mechanism involves the interaction of **Int1** with the 3-methylthiophene and formation of a new B–C bond *via* a transition state **TS2** at 12.0 kcal mol<sup>–1</sup>. A corresponding local minimum structure **Int2** is stable, albeit with a very similar relative energy to **TS2** ( $\Delta G_{\text{Int2-TS2}} = -0.7$  kcal mol<sup>–1</sup>). A subsequent N–B bond breakage (**TS3**) occurs easily as the barrier is only 13.5 kcal mol<sup>–1</sup>. The local minimum (**Int2**) and transition state (**TS2** and **TS3**) energies are significantly lower than the barrier for **TS1**; hence, we can determine the initial hydrogen release as the rate determining step in the catalysis. The final proton transfer from the 3-methylthiophene to form the cationic **3a** is thought to be barrierless; at least we were not able to find the corresponding transition state for this final process. Overall, the formation of product **4a** is calculated to be an exergonic process ( $\Delta G = -5.1$  kcal mol<sup>–1</sup>) corroborating well with the experimental findings.



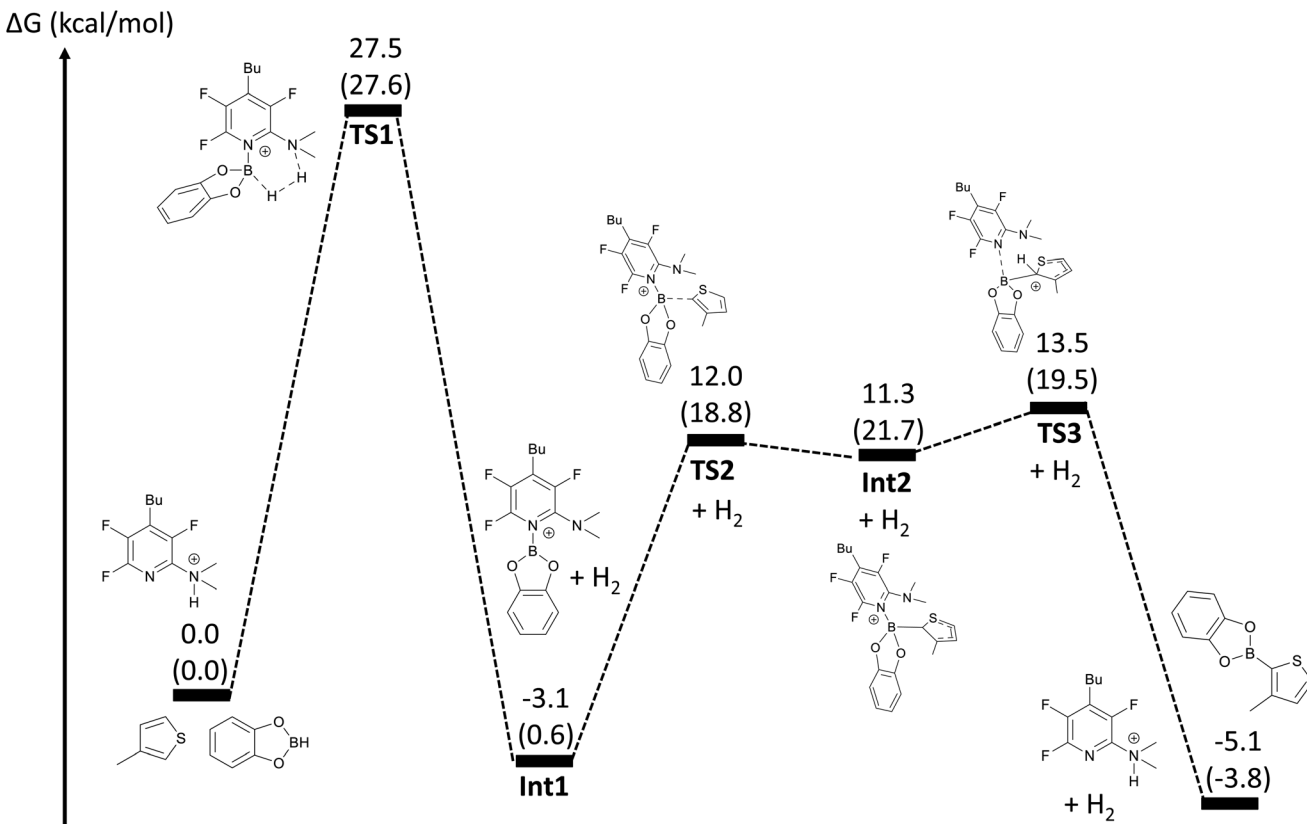


**Fig. 3** Gibbs free energy diagram of the calculated reaction mechanism. Calculations were performed for the cationic component of **3a**. The energies are given in  $\text{kcal mol}^{-1}$  in the gas phase at 298 K; the values in the parenthesis represent relative single-point energies obtained using a solvent correction (PCM = 1,2-dichloroethane).

## Conclusions

In conclusion, vital parts of the catalyst structure based on the *ortho*-*N*-substituted pyridine core were established. For such type of a borylation catalyst, there is a high requirement for electron-deficiency that can be accomplished by adding fluorine substituents in the pyridine core. According to DFT,  $\text{H}_2$  liberation is the rate-determining step in the proposed catalytic cycle. Thus, the acidic *ortho*-*N*-substituent plays a role of a “proton shell”, in which the proton has to be in an accessible orientation together with hydroborane for hydrogen liberation. Methylthiophenes and *N*-alkylbenzenes are available for  $\text{sp}^2$  C–H borylation through the described catalytic cycle using bench-stable catalyst **3a**. The reaction proceeds only with acid-resistant hydroboranes, such as CatBH. The main limitation of the studied borylation is oligomerization of CatBH as a parallel pathway. Due to CatBH and its products, the reaction has to be carried out under an air-free atmosphere, although the catalyst is bench-stable.

## Author contributions

N. S. – conceptualization, data curation, investigation, methodology, visualization, and writing – original draft. E. M. – formal

analysis and validation. J. M. P. – formal analysis, validation, methodology, and writing – review & editing. S. H. – NMR analysis and data curation. D. S. and M. N. – X-ray structure analysis, data curation, formal analysis, and visualisation. P. V. – methodology, data curation, formal analysis, and writing – review & editing. T. R. – supervision.

## Conflicts of interest

There are no conflicts to declare.

## Acknowledgements

This work has been supported by CHEMS – The Doctoral Programme in Chemistry and Molecular Sciences at University of Helsinki. PV wishes to thank the Jenny and Antti Wihuri Foundation and the Research Council of Finland (grant no. 338271 and 346565) for funding. The authors wish to acknowledge CSC – IT Center for Science, Finland for computational resources. A. Eronen is thanked for help with HRMS measurements and J. Mannisto for discussions and corrections during the preparation of the manuscript.



## References

- 1 T. Dalton, T. Faber and F. Glorius, *ACS Cent. Sci.*, 2021, **7**, 245–261.
- 2 I. A. I. Mkhald, J. H. Barnard, T. B. Marder, J. M. Murphy and J. F. Hartwig, *Chem. Rev.*, 2010, **110**, 890–931.
- 3 N. Schneider, D. M. Lowe, R. A. Sayle, M. A. Tarselli and G. A. Landrum, *J. Med. Chem.*, 2016, **59**, 4385–4402.
- 4 C.-L. Sun and Z.-J. Shi, *Chem. Rev.*, 2014, **114**, 9219–9280.
- 5 K. Chernichenko, M. Lindqvist, B. Kótai, M. Nieger, K. Sorochkina, I. Pápai and T. Repo, *J. Am. Chem. Soc.*, 2016, **138**, 4860–4868.
- 6 Q. Yin, H. F. T. Klare and M. Oestreich, *Angew. Chem., Int. Ed.*, 2017, **56**, 3712.
- 7 M.-A. Légaré, M.-A. Courtemanche, É. Rochette and F.-G. Fontaine, *Science*, 2015, **349**, 513–516.
- 8 J. Légaré Lavergne, A. Jayaraman, L. C. Misal Castro, É. Rochette and F.-G. Fontaine, *J. Am. Chem. Soc.*, 2017, **139**, 14714–14723.
- 9 É. Rochette, V. Desrosiers, Y. Soltani and F.-G. Fontaine, *J. Am. Chem. Soc.*, 2019, **141**, 12305–12311.
- 10 J. Lv, X. Chen, X.-S. Xue, B. Zhao, Y. Liang, M. Wang, L. Jin, Y. Yuan, Y. Han, Y. Zhao, Y. Lu, J. Zhao, W.-Y. Sun, K. N. Houk and Z. Shi, *Nature*, 2019, **575**, 336–340.
- 11 V. Iashin, D. Berta, K. Chernichenko, M. Nieger, K. Moslova, I. Papai and T. Repo, *Angew. Chem., Int. Ed.*, 2020, **26**, 13873–13879.
- 12 A. Del Grosso, R. G. Pritchard, C. A. Muryn and M. J. Ingleson, *Organometallics*, 2010, **29**, 241–249.
- 13 X. Tan, X. Wang, Z. H. Li and H. Wang, *J. Am. Chem. Soc.*, 2022, **144**, 23286–23291.
- 14 V. Desrosiers, A. Gaudy, K.-A. Giroux and F.-G. Fontaine, *Z. Anorg. Allg. Chem.*, 2023, **649**, e202300006.
- 15 D. W. Stephan, *Org. Biomol. Chem.*, 2008, **6**, 1535.
- 16 V. Sumerin, F. Schulz, M. Atsumi, C. Wang, M. Nieger, M. Leskelä, T. Repo, P. Pyykkö and B. Rieger, *J. Am. Chem. Soc.*, 2008, **130**, 14117–14119.
- 17 D. Stephan and G. Erker, *Angew. Chem., Int. Ed.*, 2010, **49**, 46–76.
- 18 V. Sumerin, K. Chernichenko, M. Nieger, M. Leskelä, B. Rieger and T. Repo, *Adv. Synth. Catal.*, 2011, **353**, 2093–2110.
- 19 K. Chernichenko, B. Kótai, I. Pápai, V. Zhivonitko, M. Nieger, M. Leskelä and T. Repo, *Angew. Chem., Int. Ed.*, 2015, **54**, 1749–1753.
- 20 V. V. Zhivonitko, K. Sorochkina, K. Chernichenko, B. Kótai, T. Földes, I. Pápai, V.-V. Telkki, T. Repo and I. Koptyug, *Phys. Chem. Chem. Phys.*, 2016, **18**, 27784–27795.
- 21 K. Sorochkina, V. V. Zhivonitko, K. Chernichenko, V.-V. Telkki, T. Repo and I. V. Koptyug, *J. Phys. Chem. Lett.*, 2018, **9**, 903–907.
- 22 J. Zheng, Z. H. Li and H. Wang, *Chem. Sci.*, 2018, **9**, 1433–1438.
- 23 C. Mömeling, E. Otten, G. Kehr, R. Fröhlich, S. Grimme, D. Stephan and G. Erker, *Angew. Chem., Int. Ed.*, 2009, **48**, 6643–6646.
- 24 I. Peuser, R. C. Neu, X. Zhao, M. Ulrich, B. Schirmer, J. A. Tannert, G. Kehr, R. Fröhlich, S. Grimme, G. Erker and D. W. Stephan, *Chem. – Eur. J.*, 2011, **17**, 9640–9650.
- 25 D. Voicu, M. Abolhasani, R. Choueiri, G. Lestari, C. Seiler, G. Menard, J. Greener, A. Guenther, D. W. Stephan and E. Kumacheva, *J. Am. Chem. Soc.*, 2014, **136**, 3875–3880.
- 26 M.-A. Légaré, M.-A. Courtemanche and F.-G. Fontaine, *Chem. Commun.*, 2014, **50**, 11362–11365.
- 27 V. Bagutski, A. Del Grosso, J. A. Carrillo, I. A. Cade, M. D. Helm, J. R. Lawson, P. J. Singleton, S. A. Solomon, T. Marcelli and M. J. Ingleson, *J. Am. Chem. Soc.*, 2013, **135**, 474–487.
- 28 É. Rochette, M. Courtemanche and F. Fontaine, *Chem. – Eur. J.*, 2017, **23**, 3567–3571.
- 29 A. Prokofjevs and E. Vedejs, *J. Am. Chem. Soc.*, 2011, **133**, 20056–20059.
- 30 C.-C. Han, *et al.*, *United States Patent Application Publication*, US2014/0293514A1, 2014.
- 31 S. A. Westcott, H. P. Blom, T. B. Marder, R. T. Baker and J. C. Calabrese, *Inorg. Chem.*, 1993, **32**, 2175–2182.
- 32 J. R. Lawson, E. R. Clark, I. A. Cade, S. A. Solomon and M. J. Ingleson, *Angew. Chem., Int. Ed.*, 2013, **52**, 7518–7522.
- 33 E. R. Clark, A. Del Grosso and M. J. Ingleson, *Chem. – Eur. J.*, 2013, **19**, 2462–2466.

